

Hydrogen-Bonded Dihydrotetraazapentacenes

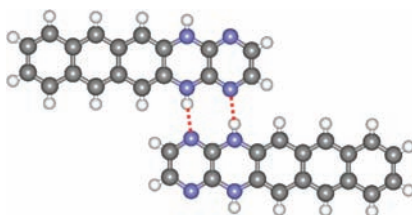
Zikai He, Danqing Liu, Renxin Mao, Qin Tang, and Qian Miao*

Department of Chemistry, the Chinese University of Hong Kong, Shatin,
New Territories, Hong Kong, China

miaoqian@cuhk.edu.hk

Received December 21, 2011

ABSTRACT



Three new members of *N*-heteropentacenes explored herein have adjacent pyrazine and dihydropyrazine rings at one end of the pentacene backbone. Interesting findings from this study include self-complementary N–H···N H-bonds in the solid state, solvent-dependent UV–vis absorption caused by H-bonding, and new *p*-type organic semiconductors with field effect mobility up to $0.7 \text{ cm}^2 \text{ V}^{-1} \text{ s}^{-1}$.

N-heteropentacenes, which have N atoms inserted into the backbone of pentacene, have recently been found as a new family of organic semiconductors with high performance in organic thin film transistors (OTFTs).¹ A combination of varied number, position, and valence state of N atoms in *N*-heteropentacenes can in principle yield a large number of structurally related π -backbones and thus provide good opportunities for developing novel organic semiconductors and studying structure–property relationship. Unlike pentacene, *N*-heteropentacenes are capable of H-bonds with N atoms. As found from the known crystal structures, *N*-heteropentacenes can form not only classical H-bonds (N–H···O and N···H–O) with solvent molecules,^{2,3} but also weak H-bonds (C–H···N) with each other.⁴ Because of the greater strength, classical H-bonds are in principle more powerful in directing the molecular packing of *N*-heteropentacenes. However, classical H-bonds between *N*-heteropentacene molecules have not been reported to the best of our knowledge.

To explore how classical H-bonds (N–H···N) tune the properties of *N*-heteropentacenes, we designed a new

dihydrotetraazapentacene (**1**) that has adjacent pyrazine and dihydropyrazine rings at one end of the pentacene backbone as shown in Figure 1. This design allows self-complementary N–H···N H-bonds in the solid state as detailed in this letter. Following the success of silylethynylated pentacene⁵ and *N*-heteropentacenes^{4,6} as soluble and stable organic semiconductors with high charge carrier mobility, triisopropylsilylethynyl groups are introduced to **1** leading to **2** and **3**. Particularly, the NH groups of **2** are exposed as found from the space-filling model shown in Figure 1b and thus are available for H-bonding. On the other hand, the NH groups of **3** are shielded by the bulky triisopropylsilyl groups and thus are unavailable or at least much less available for H-bonds with a H-bond acceptor. Studying UV–vis absorption of **2** and **3** in different solvents has led to an interesting finding on solvent-dependent absorption caused by H-bonding. It is found that both **1** and **3** function as *p*-type organic semiconductors in thin film transistors, and **3** exhibits field effect mobility as high as $0.7 \text{ cm}^2 \text{ V}^{-1} \text{ s}^{-1}$.

Shown in Scheme 1 are the syntheses of **1–3** in two ways. **1** and **2** were synthesized from 2,3-diaminopyrazine

(1) Miao, Q. *Synlett* **2012**, in press (DOI: 10.1055/s-0031-1290323).
(2) Miao, Q.; Nguyen, T.-Q.; Someya, T.; Blanchet, G. B.; Nuckolls, C. *J. Am. Chem. Soc.* **2003**, *125*, 10284.
(3) Tang, Q.; Liu, J.; Chan, H. S.; Miao, Q. *Chem.—Eur. J.* **2009**, *15*, 3965.
(4) Liang, Z.; Tang, Q.; Mao, R.; Liu, D.; Xu, J.; Miao, Q. *Adv. Mater.* **2011**, *23*, 5514.

(5) Anthony, J. E. *Angew. Chem., Int. Ed.* **2008**, *47*, 452.
(6) (a) Liu, Y.-Y.; Song, C.-L.; Zeng, W.-J.; Zhou, K.-G.; Shi, Z.-F.; Ma, C.-B.; Yang, F.; Zhang, H.-L.; Gong, X. *J. Am. Chem. Soc.* **2010**, *132*, 16349. (b) Liang, Z.; Tang, Q.; Xu, J.; Miao, Q. *Adv. Mater.* **2011**, *23*, 1535. (c) Song, C. L.; Ma, C.-B.; Yang, F.; Zeng, W.-J.; Zhang, H.-L.; Gong, X. *Org. Lett.* **2011**, *13*, 2880. (d) Wang, C.; Liang, Z.; Liu, Y.; Wang, X.; Zhao, N.; Miao, Q.; Hu, W.; Xu, J. *J. Mater. Chem.* **2011**, *21*, 15201.

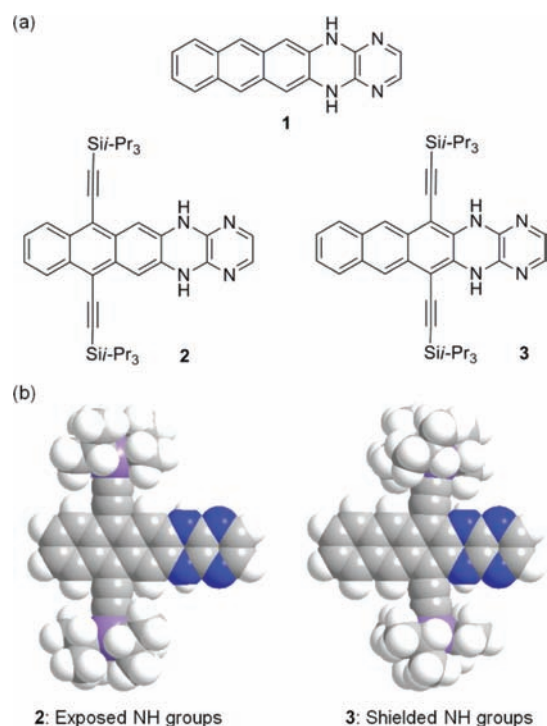


Figure 1. (a) Molecular structures of 5,14-dihydro-1,4,5,14-tetraazapentacene (**1**) and its ethynylated derivatives (**2** and **3**). (b) Space-filling models of **2** and **3** as optimized at B3LYP/6-31g(d,p) level of density functional theory (DFT) (C, N, Si, and H atoms are shown in gray, blue, violet, and white, respectively).

and the corresponding dihydroanthranenes (**4**² and **5**, respectively) by solvent-free condensation at 205–215 °C. The new compound **5** was prepared from 2,3-dimethoxyanthracene² in five steps as detailed in the Supporting Information. The low yield of **2** may be attributed to the low stability of **5** at high temperature. Unlike its constitutional isomer **2**, **3** was synthesized by Pd-catalyzed coupling of **6**⁷ and 2,3-dichloropyrazine using 1,1'-bis(diphenylphosphino)ferrocene (dppf) as ligand and Cs₂CO₃ as base. This condition was a modification from Bunz's recent synthesis⁸ of an isomer of **2** and **3** from 2,3-dichloroquinoxaline and 1,4-bis(triisopropylsilylethynyl)-2,3-diaminonaphthalene using biaryl phosphane ligand and Hünig's base.

Molecules **1**–**3** may each in principle exist as three isomers by varying the position of H atoms that are bonded to N atoms. As the representative, the three isomers of **1** are shown in Figure 2. According to Clar's aromatic sextet rule,⁹ **1** is more energetically favorable than **1'** and **1''** because **1** has two aromatic sextet rings, while **1'** and **1''** have only one. The ¹H NMR of **1** shows four singlet peaks and two sets of peaks

Scheme 1. Synthesis of **1**–**3**

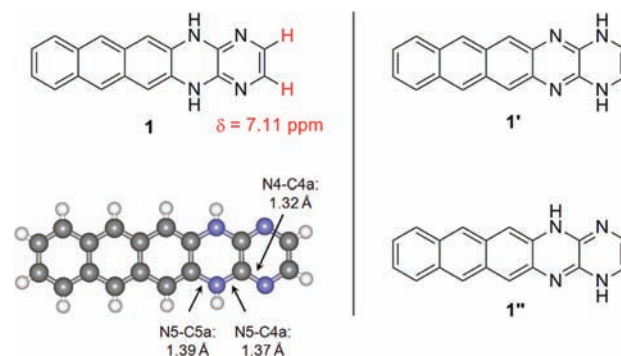
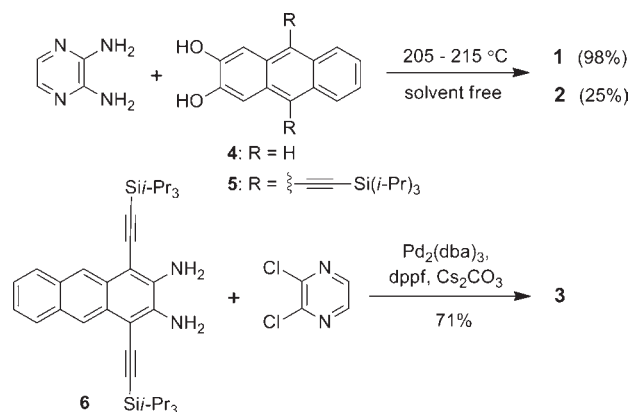


Figure 2. Possible isomeric structures of **1** and the crystal structure of **1** (C, N, and H atoms are shown in gray, blue, and white, respectively).

with characteristic AA'XX' patterns, in agreement with the C_{2v} symmetry, thus excluding the structure of **1''**. Moreover, the H2 and H3 of **1** (shown in red in Figure 2) exhibit a chemical shift at 7.11 ppm, which is very close to the chemical shift (7.13 ppm) of the corresponding H atoms in 2,3-diaminopyrazine.¹⁰ As shown in Figure 2, the N5–C5a and N5–C4a bonds are both longer than the N4–C4a bond, and the N5–C5a bond has the same length as the N–C bond (1.39 Å) in 6,13-dihydro-6,13-diazapentacene.² These bond lengths support the structure of **1**, which has dihydropyrazine as the second ring.

Compound **1** is only soluble in DMSO and DMF, while **2** and **3** are soluble in a variety of organic solvents including benzene, CH₂Cl₂, acetone, and THF. Dissolving **2** and **3** in varied solvents has led to an interesting finding that **2** exhibits an apparent solvent-caused color change, while **3** almost keeps the same color in different solvents. As shown in Figure 3a, a solution of **2** in CH₂Cl₂ appears yellow, but that in DMSO appears orange. This color change is accompanied with a red shift of longest-wavelength

(7) Appleton, A. L.; Brombosz, S. M.; Barlow, S.; Sears, J. S.; Bredas, J.-L.; Marder, S. R.; Bunz, U. H. F. *Nat. Commun.* **2010**, *1*, 91 (DOI: 10.1038/ncomms1088).

(8) Tverskoy, O.; Rominger, F.; Peters, A.; Himmel, H.-J.; Bunz, U. H. F. *Angew. Chem., Int. Ed.* **2011**, *50*, 3557–3560.

(9) (a) Clar, E. *The Aromatic Sextet*; Wiley: New York, 1972. (b) Harvey, R. G. *Polycyclic Aromatic Hydrocarbons*; Wiley-VCH: New York, 1997.

(10) The ¹H NMR spectra of **1** and 2,3-diaminopyrazine were both measured in DMSO-*d*₆.

absorption by 35 nm. Such solvent-dependent color change may possibly be related to solvatochromism, which is a well-known phenomenon of color change due to a change in solvent polarity. The widely accepted explanation for solvatochromism is that the ground state and the Franck–Condon excited state of a polar chromophore are stabilized by polar solvent molecules with different degree.¹¹ To determine whether the solvent-caused color change of **2** is a solvatochromic effect, the absorption spectra of **2** were recorded in varied solvents. As shown in Figure 3b, the measured values of longest-wavelength absorption were first plotted against the dielectric constant of the corresponding solvent. The data for **2** show neither positive nor negative correlation between the longest-wavelength absorption and the solvent dielectric constant, indicating that the solvent-caused color change of **2** can not be described with classical solvatochromism.

On the other hand, the chemical shift for N–H of **2** exhibits a downfield shift from 6.81 ppm to 10.49 ppm when the solvent changes from CD_2Cl_2 to $\text{DMSO-}d_6$, indicating formation of H-bonds between **2** and DMSO. To test the effect of H-bonding on absorption, the measured values of longest-wavelength absorption were plotted against the solvent H-bond basicity parameter ($\text{p}K_{\text{HB}}$)¹² as shown in Figure 3c. The positive correlation presented in Figure 3c indicates that the solvent-caused color change of **2** in fact depends on the H-bond basicity of solvents. This dependence can be understood in terms of the H-bonded complex **2**·2Sol and its resonance form **2'**·2Sol as shown in Figure 3d. The resonance form **2'** is expected to contribute to the longer-wavelength absorption because it has a diazatetracene substructure with greater conjugation. Therefore, the factors that stabilize **2'** can lead to a red shift of absorption band. The higher H-bond basicity a solvent has, the stronger H-bond it forms with **2**. A stronger H-bond weakens the N–H bond by a greater degree, leading to a more negative charge on the N atoms. Such H-bond-induced negative charge can partially counterbalance the positive charge on N atoms in **2'** and thus stabilize this resonance form. As stabilized by stronger H-bonds, **2'** can make greater contribution to the resonance structure of **2**, leading to red-shifted absorption. In contrast, the longest-wavelength absorption of **3** only exhibits a very small red shift when the solvent is changed from CH_2Cl_2 to DMSO as shown in Figure 3c because its shielded N–H groups are much less available, if not unavailable, for H-bonds with solvent molecules.

Single crystals of **1** and **3** were grown by physical vapor transport and from solution in ethyl acetate, respectively. X-ray crystallographic analysis on the single crystals of **1** and **3** has revealed their molecular packing. Molecules of **1** form H-bonded ribbons, which stack in two directions. As shown in Figure 4a, molecules of **1** are linked by double N–H···N H-bonds, which have the N-to-N distance

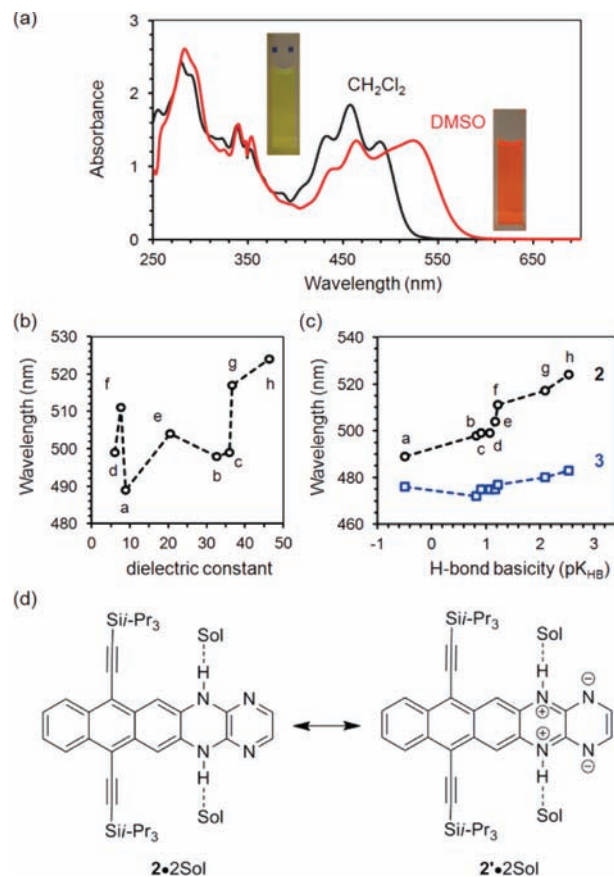


Figure 3. (a) Absorption spectra of **2** in CH_2Cl_2 and DMSO (5×10^{-5} mol/L). (b) The longest-wavelength absorption of **2** in varied solvents versus the dielectric constant of solvent (a: CH_2Cl_2 , b: CH_3OH , c: CH_3CN , d: ethyl acetate, e: acetone, f: THF, g: DMF, h: DMSO). (c) The longest-wavelength absorption of **2** and **3** in varied solvents versus the H-bond basicity of solvent. (d) Resonance structures for H-bonded complex of **2** and solvent molecules (Sol).

of 3.05 Å, the H-to-N distance of 2.25 Å, and the N–H–N angle of 154.7°. Two π -stacked molecules of **1** are separated by a distance of 3.42 Å between π -planes and have an offset arrangement with a relative shift along the long molecular axis. In the crystal lattice, each molecule of **1** occupies a volume of 320.14 Å³, which is smaller than the volume occupied by 6,13-dihydro-6,13-diazapentacene (332.15 Å³ per molecule)² and 6,13-diazapentacene (333.89 Å³ per molecule).¹³ This suggests that H-bonds between *N*-heteropentacene molecules can be helpful in forming denser packing. As shown in Figure 4b, **3** exhibits π -stacking of two-dimensional brickwork arrangement, which is typical of silylethynylated pentacenes⁵ and *N*-heteropentacenes.^{4,6} The distance between π planes of **3** is 3.35–3.37 Å. No H-bonds are found between molecules of **3** in the crystal structures in agreement with the shielded NH groups.

Semiconductor properties of **1** and **3** were tested in vacuum-deposited thin film transistors, which have octadecyltrimethoxysilane (OTMS) modified 300 nm-thick

(11) Reichardt, C.; Welton, T. *Solvents and Solvent Effects in Organic Chemistry*, 4th ed.; Wiley-VCH: Weinheim, Germany, 2011.

(12) Lamarche, O.; Platts, J. A. *Chem.—Eur. J.* **2002**, *8*, 457. (b) Ouvrard, C.; Berthelot, M.; Laurence, C. *J. Chem. Soc., Perkin Trans. 2* **1999**, *7*, 1357.

(13) Miao, Q. Ph.D. Thesis, Columbia University: New York, 2005.

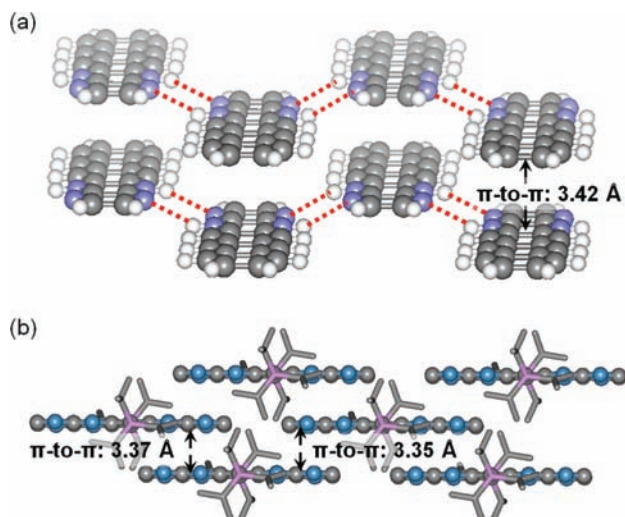


Figure 4. Molecular packing of **1** and **3** in crystals: (a) H-bonds (shown as red dashed lines) and π -stacks of **1**; (b) brickwork π -stacks of **3**. The *N*-heteropentacene cores are shown as ball-stick model and the silylethynyl substituents are shown in stick model. H atoms are removed for clarification. The grayish-blue colored atoms of **3** contain both N and C atoms due to disorder.

SiO₂ as dielectrics,¹⁴ vacuum-deposited gold as top-contact drain and source electrodes, and heavily doped silicon as a bottom gate electrode. However, efforts to fabricate devices from **2** by thermal evaporation failed because it decomposed during heating under vacuum. The X-ray diffractions (XRD) from the films of **1** did not show any peaks indicating the amorphous nature of **1** in the film. On the other hand, XRD from **3** (shown in the Supporting Information) exhibited four peaks in accordance with the (001), (002), (003), and (005) diffractions derived from the single crystal structure, indicating a highly crystalline film. It is found that both **1** and **3** function as *p*-type semiconductors with field effect mobility of $4\text{--}7 \times 10^{-4}$ and $0.3\text{--}0.7 \text{ cm}^2 \text{ V}^{-1} \text{ s}^{-1}$, respectively. The *p*-type semiconductor behaviors of **1** and **3** are in agreement with their energy levels of highest occupied molecular orbital (HOMO) at -4.80 eV and -5.17 eV , respectively, which were estimated from the irreversible oxidation waves in the cyclic voltammograms (see the Supporting Information). The low field effect mobility of **1** should be attributed to the amorphous nature of its vacuum-deposited film, as it is well-known that the field effect mobility is very sensitive to the crystallinity of the thin

(14) Ito, Y.; Virkar, A. A.; Mannsfeld, S.; Oh, J. H.; Toney, M.; Locklin, A.; Bao, Z. *J. Am. Chem. Soc.* **2009**, *131*, 9396.

(15) Dimitrakopoulos, C. D.; Malenfant, P. R. L. *Adv. Mater.* **2002**, *14*, 99.

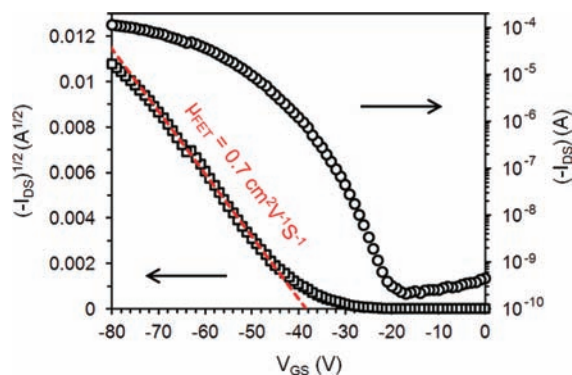


Figure 5. Drain current (I_{DS}) versus gate voltage (V_{GS}) at drain voltage (V_{DS}) of -80 V for an OTFT of **3** with the active channel of $W = 1 \text{ mm}$ and $L = 50 \mu\text{m}$ as measured in air.

film.¹⁵ The disordered arrangement of **1** in the thin films prevents evaluating the effect of H-bonding on charge transport by comparing the field effect mobility of **1** with those of other *N*-heteropentacenes that do not form H-bonds in the solid state. Shown in Figure 5 are the transfer I - V curves for the best-performing OTFT of **3**, which exhibits a field-effect mobility of $0.7 \text{ cm}^2 \text{ V}^{-1} \text{ s}^{-1}$ and an on/off ratio of 3×10^5 for drain current between 0 and -80 V gate bias.

In conclusion, the above study has explored three new members of *N*-heteropentacenes that have adjacent pyrazine and dihydropyrazine rings at one end of the pentacene backbone. This design not only allows self-complementary $\text{N-H}\cdots\text{N}$ H-bonds in the solid state, but also leads to interesting findings on solvent-dependent UV-vis absorption, which can be attributed to H-bonds with solvent molecules. Two of the compounds are found to function as *p*-type semiconductors in OTFTs. Further investigation on single-crystal transistors of **1** may allow evaluating the effect of H-bonding on charge transport.

Acknowledgment. This work was supported by grants from the Research Grants Council of Hong Kong (Project No. GRF402508 and CUHK2/CRF/08).

Supporting Information Available. Details of synthesis, cyclic voltammetry, UV-vis absorption, DFT calculation, fabrication and characterization of thin film transistors, NMR spectra, and CIF files for **1** and **3**. This material is available free of charge via the Internet at <http://pubs.acs.org>.

The authors declare no competing financial interest.